# How does the OH reactivity affect the ozone production efficiency: case studies in Beijing and Heshan, China

Yudong Yang[1], Min Shao[1, *], Stephan. Keβel[2], Yue Li[1], Keding Lu[1], Sihua Lu[1], Jonathan Williams[2], Yuanhang Zhang[1], Liming Zeng[1], Anke C. Nölscher[2, #], Yusheng Wu[1], Xuemei Wang[3], Junyu Zheng[4],

[1] State Joint Key Laboratory of Environmental Simulation and Pollution Control, College of Environmental Science and Engineering, Peking University, Beijing, China
[2] Department of Atmospheric Chemistry, Max Plank-Institute for Chemistry, Mainz, Germany
[3] School of Atmospheric Science, Sun Yat-Sen University, Guangzhou, China
[4] School of Environmental Science and Engineering, South China University of Technology, China
# now at: Division of Geological and Planetary Sciences, California Institute of Technology, Pasadena, USA

* Corresponding to: Min Shao
Email address: mshao@pku.edu.cn

## Abstract

Total OH reactivity measurements were conducted on the Peking University campus, Beijing in August 2013 and in Heshan, Guangdong Province from October to November 2014. The daily median OH reactivity were 20 ± 11 $s^{-1}$ in Beijing and 31 ± 20 $s^{-1}$ in Heshan respectively. The data in Beijing showed a distinct diurnal pattern with the maxima over 27 $s^{-1}$ in early morning and minima below 16 $s^{-1}$ in the afternoon. The diurnal pattern in Heshan was not as evident as in Beijing. Missing reactivity, defined as the difference between measured and calculated OH reactivity, was observed at both sites, with 21% missing in Beijing and 32% missing in Heshan. Unmeasured primary species, such as branched-alkenes could contribute to missing reactivity in Beijing, especially in morning rush hours. An observation-based model with the RACM-2 (Regional Atmospheric Chemical Mechanism version 2) was used to understand the daytime missing reactivity in Beijing by adding unmeasured oxygenated volatile organic compounds and simulated intermediates of the degradation from primary VOCs. However, the model could not find the convincing

explanation for the missing in Heshan, where the ambient air was found to be more aged, and the missing reactivity was presumably attributed to oxidized species, such as unmeasured aldehydes, acids and di-carbonyls. The ozone production efficiency was 21% higher in Beijing and 30% higher in Heshan when the model was constrained by the measured reactivity, compared to the calculations with measured and modeled species included, indicating the importance of quantifying the OH reactivity for better understanding ozone chemistry.

## 1. Introduction

Studies on total OH reactivity in the atmosphere have been of increasing interest over the last two decades. The instantaneous total OH reactivity, is defined as

$$k_{OH} = \sum_i k_{OH+X_i}[X_i] \quad (1\text{-}1)$$

where X represents a reactive species (CO, $NO_2$ etc.) and $k_{OH+X_i}$ is the rate coefficient for the reaction between X and OH radicals. Total OH reactivity is an index for evaluating the amounts of reductive pollutants in terms of ambient OH loss and hence their roles in atmospheric oxidation (Williams, 2008; Williams and Brune, 2015; Yang et al., 2016). It also provides a constraint for OH budget calculation in both field campaigns and laboratory studies (Stone et al., 2012; Fuchs et al., 2013).

Total OH reactivity measuring techniques, e.g., two laser-induced-fluorescence (LIF) based techniques (Calpini, et al., 1999; Kovacs and Brune, 2001) and one proton-transfer-reaction mass spectrometry (PTR-MS) based technique, comparative reactivity method (CRM) (Sinha et al., 2008) were developed in recent years. A brief comparison of these techniques and their interferences were summarized (Yang et al., 2016). By deploying these measuring techniques, total OH reactivity measurements have been intensively conducted in urban and suburban areas. Details of these campaigns were listed in Table 1 and Table 2. Most of the campaigns exhibited similar diel features with higher reactivity in dawn and rush hours of early morning, and lower levels in the afternoon, which could be explained by the change in

boundary layer height, emissions and oxidation processes. Anthropogenic volatile organic compounds (VOCs) and inorganics, such as CO and $NO_x$ (NO + $NO_2$) are major known OH sinks in urban areas.

However, a substantial difference between measured and calculated or modelled OH reactivity, termed as the missing reactivity, was revealed in most field campaigns. Compared to the high percentages of missing reactivity in forested areas (Sinha et al., 2010; Nölscher et al., 2012; 2016; Edwards et al., 2013, Williams et al., 2016), most campaigns in urban and suburban areas gave relatively lower percentages of missing reactivity except for the 75% missing reactivity in Paris in MEGAPOLI under the influences of continental air masses (Dolgorouky et al, 2012).

Various methods were used in exploring the origins of missing reactivity. Unmeasured primary species are important candidates. Sheehy et al. (2010) discovered a higher percentage of missing reactivity in morning rush hours and found that the unmeasured primary species, including organics with semi and low-volatility, could contribute up to 10% of total reactivity. Direct measurements on reactivity of anthropogenic emission sources were conducted, such as vehicle exhaust and gasoline evaporation. An average of 17.5% missing reactivity was found in vehicle exhaust measurements (Nakashima et al., 2010). For gasoline evaporation, a study showed that if primary emitted branched-chained alkenes were considered, the measured and calculated reactivity then agreed (Wu et al., 2015). Besides primary emitted species, unknown secondary species were not negligible. Yoshino et al. (2006) found a good correlation between missing reactivity and measured oxygenated VOCs (OVOCs) in three seasons except for winter, assuming that the unmeasured OVOCs could be major contributors of missing reactivity, in one case the OVOCs could increase reactivity by over 50% (Lou et al., 2010). The observation-based model (OBM) was widely used to evaluate the measured reactivity (Lee et al., 2010; Lou et al., 2010; Whalley et al., 2016), confirming the important contribution from OVOCs and undetected intermediate compounds,.

Ground-level ozone pollution has been of increasing concerns in China. While the ozone concentration exceeds Grade II of China National Ambient Air Quality

Standards (2012) (93 ppbV) frequently in summer in Beijing-Tianjin-Hebei area and Pearl River Delta (PRD) region (Wang et al., 2006; Zhang et al., 2008), it appears there is an increasing trend for ozone in Beijing and other area recent years (Zhao et al., 2009; Zhang et al., 2014). Comparing to traditional empirical kinetic model approach (EKMA) (Dodge et al., 1977), the OH reactivity due to VOCs (termed as VOCs reactivity) rather than VOCs mixing ratio was used in the calculation of ozone production rate (Geddes et al., 2009; LaFranchi et al., 2011; Sinha et al, 2012; Zhang et al., 2014). Due to the limitation of current measurement techniques, some VOCs species which could not be quantified so far, and therefore cannot be integrated into current chemical mechanisms of model run, could laid a great uncertainty in ozone production prediction. By directly measuring the total OH reactivity, VOCs reactivity can be obtained by deducting the inorganic reactivity from the total OH reactivity, which provides a constrain for evaluating the roles of reactive VOCs in air chemistry (Sadanaga et al, 2005; Sinha et al, 2012; Yang et al., 2016).

This paper presents field data in China from two intensive observation conducted in August 2013 in Beijing, and October to November 2014 in Heshan, Guangdong, focusing on OH reactivity and related species. The variations of total OH reactivity at both sites were compared with similar observations in urban and suburban areas worldwide. Thereafter, a zero dimensional box model based on Regional Atmospheric Chemical Mechanism 2 (RACM2) was employed for OH reactivity simulations. The possible missing reactivity and its importance for the ozone production calculation are discussed.

# 2. Methods

## 2.1 Total OH reactivity measurements

### 2.1.1 Measurement principles

Total OH reactivity was measured by the comparative reactivity method (CRM) first developed at Max Planck Institute for Chemistry (Sinha et al., 2008). The CRM system was built accordingly in Peking University, which consisted of 3 major components: inlet and calibration system, reactor, and measuring system as shown in

Fig 1. Ambient air was sampled after a teflon filter and then pumped through a 14.9m Teflon 3/8 inch (outer diameter) inlet at about 7 $L \cdot min^{-1}$ rate, with a 5 - 6 s residence time.

In this method, pyrrole ($C_4H_5N$) was used as the reference substance and was quantified by a quadrupole PTR-MS (Ionicon Analytic, Austria). There are 4 working modes for measuring procedure: In the C0 mode, pyrrole (Air Liquid Ltd, U.S.) is introduced into the reactor with dry synthetic air (99.99%, Chengweixin Gas Ltd, China). A mercury lamp (185nm, used for OH radicals generation) is turned off and high-pure dry nitrogen (99.99%, Chengweixin Gas Ltd, China), is mixed into the reactor through a second arm. In this mode, the highest signals of m/z 68 (protonated mass of pyrrole) c0 are obtained. Then in the C1 mode, the nitrogen and synthetic air is still dry but the mercury lamp is turned on. The mixing ratio of pyrrole decreased to c1. The difference between c0 and c1 is mainly due to the photolysis of pyrrole (Sinha et al., 2008). C2 mode is the "zero air" mode in which synthetic air and nitrogen are humidified before being introduced into the reactor. The photolysis of water vapor generates OH radicals which react with pyrrole in the reactor to c2 level. Then C3 mode is the measuring mode in which the automatic valve switches from synthetic air to ambient air. The ambient air is pumped into the reactor to react with OH radicals, competing with pyrrole molecules. The mixing ratio of pyrrole is detected as c3. Total OH reactivity is calculated as below, based on equations from Sinha et al. (2008):

$$k_{OH} = c1 \times k_{Pyr+OH} \times \frac{c3-c2}{c1-c3} \quad (2\text{-}1)$$

Ambient air or synthetic air was introduced at 160 -170 ml $min^{-1}$ with the total flow 320 – 350 ml $min^{-1}$(The typical dilution factor was about 2-2.15 depending on the situation). The residence time of air inside the reactor was less than 30 s before they were pumped by the Teflon pump. The typical c1 mixing ratio for pyrrole in Beijing and Heshan measurements were about 60 ppbV and 55 ppbV, while the mixing ratios of OH radicals generated by mercury lamp were about 35 ppbV and 28 ppbV. The mixing ratios were quite consistent for either of the campaigns, respectively. Corrections about pseudo-first order kinetics were conducted for both

152 measurements, based on the methods in Sinha et al (2008). The typical correction
153 factors could be presented as

154 $$R_{true} = 0.0008 * (R_{mea})^2 + 0.78 * R_{mea} - 0.042 \quad (2\text{-}2)$$

155 $$R_{true} = -0.0004 * (R_{mea})^2 + 0.81 * R_{mea} - 0.017 \quad (2\text{-}3)$$

156 **2.1.2 Calibrations and tests**

157 We performed two calibrations for the measurements. First, PTR-MS was
158 calibrated by diluted dry pyrrole standard gas ranging from less than 10 ppbV to over
159 160 ppbV (presented in Fig S1). Additionally, we conducted an inter-comparison with
160 humidified pyrrole dilution gas. The sensitivity was about 3% to 5% higher than dry
161 calibration, which was considered for later calculation (Sinha et al., 2009). The tests
162 of the CRM system were done by using both the single standard gas, such as CO,
163 propane, propene (Huayuan Gas Ltd, China) and a standard of the mixture of 56
164 non-methane hydrocarbons (NMHCs) (SpecialGas Ltd, U.S.). The results of the
165 calibrations and tests were presented in Fig 2. Measured and calculated OH reactivity
166 agreed well within the uncertainty for all calibrations.

167 A key factor influencing the measurement results is the stability of OH radical
168 generator. One major interference could be the difference in relative humidity
169 between C2 mode and C3 mode. During the experiment, we used one single needle
170 valve to control the flow rate of synthetic air going through the bubbler, so that the
171 relative humidity during C2 mode could be adjusted to match humidity during
172 ambient sampling (C3 mode). Meanwhile, the remaining minor difference could be
173 corrected by factors derived from the OH reactivity-humidity correction experiment.
174 The details of the OH-correction experiment and the data were presented in the
175 supporting information (Fig. S1 and S2).

176 The other interference might be caused by ambient NO, which produces
177 additional OH radicals via recycling of $HO_2$ radicals (Sinha et al., 2008; Dolgorouky
178 et al., 2012; Michoud et al., 2015). The amount of OH radical through this pathway is
179 hard to be quantified. In the morning rush hours or on polluted cloudy days, NO
180 levels could rise to over 30 ppbV in both Beijing and Heshan, which could then
181 potentially introduce high uncertainties for measurements. The NO-correction

experiments were conducted by introducing given amounts of VOCs standard gases into the reactor. When the stable concentrations for c2 were reached, different levels of NO were injected into the reactor and the "measured" reactivity decreased as the NO mixing ratio increased. Then a correction curve was fitted between the differences in reactivity and NO mixing ratios. Several standard gases and different levels of base reactivity (from less than $30s^{-1}$ to over $180s^{-1}$) have been tried and the curve was quite consistent for all tested gases, as shown in Fig 3. The correction derived from the curve was used later to correct ambient measurements according to simultaneous detected NO levels. The correction was necessary when NO mixing ratio was larger than 5 ppbV, which was quite often observed in the morning time as well as cloudy days in Beijing and Heshan. The relative change for reactivity results could be over 100 $s^{-1}$ when NO mixing ratio was about 30 ppbV.

A further potential interference comes from nitrous acid (HONO). The photolysis of HONO in the reactor could generate the same amount of OH radicals and NO molecules, as shown in R1. The additional OH radicals and NO molecules can be both interferences with the reactivity measurements. Similar correction experiments were conducted as the NO correction experiment. HONO were added stepwise in several mixing ratios (1-10 ppbV), generated by a HONO generator (Liu et al., 2016) and thus introduced into the reactor. A curve was fitted between the differences in reactivity and HONO mixing ratios, as presented in Fig 4. The correction associated with this curve was also applied later in the ambient measurements.

$$HONO \xrightarrow{h\nu} OH+NO \qquad (R1)$$

To make sure the production of OH radicals was stable during the experiments, C1 mode was measured for 1-2 hour every other day and C2 mode was measured for 20-30 minutes every two hours. With above calibrations and tests into consideration, the detection limits of CRM methods in two campaigns was around 5 $s^{-1}$ ($2\sigma$). The total uncertainty of the method was about 20% ($1\sigma$), due to rate coefficient of pyrrole reactions (15%), flow fluctuation (3%), instrument precision (6% when measured reactivity > 15 $s^{-1}$), standard gases (5%) and corrections for relative humidity (5%).

## 2.2 Field measurements

### 2.2.1 Measuring sites and periods

The urban measurements started from August 10$^{th}$ to August 27$^{th}$, 2013 at Peking University (PKU) Site (116.18°E, 39.99°N), which was set on the roof of a 6-floor building. The site is about 300 m from the 6-lanes road to the east and 500 m to the 8 -lanes road to the south. This site is an urban site used for intensive field measurements of air quality in Beijing for long. Detailed information about this site can be found elsewhere (Yuan et al., 2012).

Suburban measurements were conducted from October 20$^{th}$ to November 22$^{nd}$ 2014 at Heshan (HS) site, Guangdong (112.93°E, 22.73°N). The site is located on top of a small hill (60 m above ground) in Jiangmen, which is 50km from a medium size city Foshan (with a population of about 7 million) and 80 km from a megacity Guangzhou. This is the super-site for measurements of air quality trends by Guangdong provincial government, detailed information about which can also be found in Fang et al (2016).

### 2.2.2 Simultaneous measurements

During both intensive campaigns, fundamental meteorological parameters and trace gases were measured simultaneously. Meteorological parameters, such as temperature, relative humidity, pressure, wind speed, wind direction were measured. NO and $NO_x$ mixing ratios were measured by chemi-luminescence (model 42i, Thermo Fischer Inc, U.S.), and $O_3$ was measured by UV absorption (model 49i, Thermo Fischer Inc, U.S.). CO was measured by Gas Filter Correlation (model 48i, Thermo Fischer Inc, U.S.), and $SO_2$ was measured by pulsed fluorescence (model 43C, Thermo Fischer Inc, U.S.). The photolysis frequencies were measured by a spectral radiometer (SR) including 8 photolysis parameters. These parameters were all averaged into 1-minute resolution. The performances of these instruments were presented in Table S1 and Table S2.

VOCs were measured by a cryogen-free online GC-MSD/FID system, developed by Peking University (Yuan et al., 2012; Wang et al., 2014a). The time resolution is 1

hour but the sampling time starts from the 5th minute to 10th minute every hour. The system was calibrated by two sets of standard gases: 56 NMHCs including 28 alkanes, 13 alkenes and alkynes, 15 aromatics; EPA TO-15 standards (http://www.epa.gov/ttnamti1/les/ambient/airtox/to-15r.pdf), including additional OVOCs and halocarbons. The detection limits ranged from 10ppt-50ppt, depending on the species. Formaldehyde was measured by the Hantzsch method with time resolution of 1 minute. Detailed information about this instrument is described in one previous paper (Li et al., 2014).

### 2.3 Model description

#### 2.3.1 Box model

A zero-dimensional box model was applied to produce the unmeasured secondary products and OH reactivity for both field observations. The chemical mechanism employed in the model was RACM2 (Stockwell et al., 1997, Goliff et al., 2013), with implementation of Mainz Isoprene Mechanism (MIM, Pöschl et al., 2000) and update versions by Geiger et al. (2003) and Karl et al. (2006) for isoprene reactions. The model was constrained by measured photolysis frequencies, ancillary meteorology and inorganic gases measurements, as well as VOCs data. Mixing ratios of methane and $H_2$ were set to be 1.8 ppmV and 550 ppbV. The model was calculated in a time-dependent mode with 5-min time resolution. Each model run started with 3 days spin-up time to reach steady-state conditions for long-lived species. Different scenarios with 1 day, 2 days and 3 days spin-up time have been tried while the differences were within 10%. Additional loss by dry deposition was assumed to have a corresponding lifetime of 24 hours to avoid the accumulation of secondary productions. The boundary layer height was set as constant as 1000 m in the model due to the lack in measurements. This was similar to model setups in Lu et al (2013) and field measurement results in Guo et al (2016).

#### 2.3.2 Ozone production efficiency

Ozone production efficiency (OPE) is defined as the number of molecules of total oxidants produced photochemically when a molecule of $NO_x$ was oxidized (Kleinman, 2002, Chou et al., 2011). It helps to evaluate the impacts of VOCs

reactivity on ozone production in various $NO_x$ regimes. In this work, the OPE was expressed as the ratio of ozone production rate (i.e. $P(O_3)$) to $NO_x$ consumption rate (i.e. $D(NO_x)$). $NO_z$, calculated as the difference between $NO_y$ (sum of all odd-nitrogen compounds) and $NO_x$, was assumed to be the oxidation products of NOx. Thus the OPE could be also calculated as $P(O_3)/P(NO_z)$. The ozone production rate is obtained as 2-2, and the $P(NO_z)$ is approximately as production rate of $HNO_3$ as well as the production rate of organic nitrate, which is given as 2-3.

$$P(O_3) = k_{HO_2+NO}[HO_2][NO] + \sum_i k_{RO_{2_i}+NO}[RO_{2_i}][NO] \quad (2\text{-}2)$$

$$P(NO_z) = k_{NO_2+OH}[NO_2][OH] + \sum_i k_{RO_i+NO_2}[RO_i][NO_2] \quad (2\text{-}3)$$

# 3. Results

## 3.1 Time series of meteorology and trace gases

The time series of selected meteorological parameters and inorganic trace gases were presented in 5 minute averages (Fig 5). The median values of the inorganic trace gases were 0.715 ± 0.335 ppmV for CO, 6.3 ± 5.75 ppbV for NO and 36.5 ± 21.3 ppbV for $NO_2$, 57 ± 44 ppbV for $O_3$ in Beijing. In Heshan, the median results were 0.635 ± 0.355 ppmV for CO, 9.7 ± 6.95 ppbV for NO, 29.6 ± 12.6 ppbV for $NO_2$, and 55.7 ± 34.9 ppbV for $O_3$. Both results were within the range of data from literatures (Zhang et al., 2008; Zheng et al., 2010; Zhang et al., 2014). However, daytime averaged $O_3$ mixing ratio in Beijing 2013 was a little lower than the medium results (about 60 ppbV) in normal years (Zhang et al., 2014). This could be due to higher frequencies of cloudy and rainy days, which accounted for about 1/3 of our measurement duration. The measured maximum photolysis rates in cloudy/rainy days were about half of peak values of J ($O^1D$) on sunny days. Even under this circumstances, ozone levels from the campaign remained high, the pollution episodes with ozone exceeding Grade II of China National Ambient Air Quality Standards (93 ppbV) occurred quite often, and the percentage of exceedance were 40% in Beijing and 20% in Heshan.

The mixing ratios of VOCs in both campaigns were presented in Table S3 and Table S4. In summer Beijing, alkanes accounted for over 60% of the summed VOCs

mixing ratios during most of the time, while in Heshan the contribution from aromatics was 6% higher than that in Beijing. This could be explained by stronger emissions from solvent use and paint industry in the PRD region (Zheng et al., 2009). The ratio of toluene to benzene, which is typically used qualitatively as an indicator for aromatics emission sources also supported this assumption. While this ratio in Beijing was close to 2, similar to vehicle emissions (Barletta et al., 2005), the ratio in Heshan was higher than 3 due to strict control of benzene in solvent usage these days (Barletta et al., 2005; Liu et al., 2008). In the ozone polluted episode in Fig 5, the mixing ratios of most species were about twice to three times higher than the daily average results.

The diurnal variations of $NO_x$, $O_3$ and photochemical age from Beijing and Heshan site were compared in Fig 6 and Fig 7. Both sites presented similar diurnal patterns for $O_3$ and NO. However, the highest 1-hour average $O_3$ value at PKU site came in the afternoon and stayed at high level till the dawn. While $O_3$ pattern at Heshan site did not stay high in the afternoon. An additional similarity was that the NO peaks occurred at similar times for both sites. But NO decreased at a slower rate in Heshan till even 12:00 p.m. This was likely explained by the facts that the NO observed at PKU site was mainly from local vehicle emissions while $NO_x$ at Heshan site was significantly influenced by long-range transported of air masses.

VOCs measurements provided us chance to evaluate the oxidation state at two sites. Based on the OH exposure calculation methods (de Gouw et al., 2005), we chose a pair of VOCs species: m,p-xylene and ethylbenzene to calculate the photochemical age:

$$[\mathrm{OH}]\Delta t = [\ln(\frac{[E]}{[X]})_t - \ln(\frac{[E]}{[X]})_0]/(k_E - k_X) \quad (3\text{-}1)$$

Here, [E] and [X] represents the mixing ratios of ethylbenzene and m,p-xylene, $k_E$ and $k_X$ means the OH reaction rate coefficient of ethylbenzene and m,p-xylene. As presented in Fig 7, we chose 1.15 ppbV $ppbV^{-1}$ and 2.3 ppbV $ppbV^{-1}$ as emission ratios of ethylbenzene to m,p-xylene in Beijing and Heshan, as they were the largest ratios in diurnal variations for the campaign. The largest OH exposure in Beijing 2013

was calculated as $0.71 \times 10^{11}$ molecule s $cm^{-3}$ in 13:00 LTC, while the largest OH exposure in Heshan 2014 was calculated to be $1.69 \times 10^{11}$ molecule s $cm^{-3}$ in 14:00 LTC. The results in Beijing were comparable to previous reports (Yuan et al., 2012). Assuming the daytime average ambient OH concentration was $5.2 \times 10^6$ molecule $cm^{-3}$ (Lu et al., 2013), the photochemical age in Beijing was estimated to be not more than 3.5 h. With measured daytime average OH concentration as $7.5 \times 10^6$ molecule $cm^{-3}$ in Heshan (Tan et al., in preparation), the photochemical age in Heshan was about 6 h to 7 h, which was about twice the photochemical age of the Beijing observations, indicating a more aged atmospheric environment in Heshan. However, the assumed OH radical concentrations' influence on the photochemical age results should not be neglected.

### 3.2 Measured reactivity

Total OH reactivity ranged from less than 10 $s^{-1}$ to over 100 $s^{-1}$ in Beijing (Fig 5a). The daily median value was $20 \pm 11$ $s^{-1}$. The diurnal patterns changed significantly from day to day (Fig 8). The averaged diurnal pattern showed that the total OH reactivity was higher from dawn to morning rush hours with a peak hourly mean of 27 $s^{-1}$, and decreased to a lower value, median value of 17 $s^{-1}$ in the afternoon. This diurnal pattern was similar to the variations of $NO_x$ mixing ratios (Williams et al., 2016).

Meanwhile, measured total OH reactivity in Heshan was higher in median but the diel variation was less evident. The daily median value was $31 \pm 20$ $s^{-1}$. The OH reactivity was much less variable in the daily variation. This could possibly due to the more aged air masses in Heshan, as presented in 3.1. The other probable explanation could be the two periods of clean air we encountered, during which ground-level ozone and $PM_{2.5}$ concentrations were rather low, each of the cases lasted for about 5 days during our measurements. And 2 pollution episodes were identified between October 24$^{th}$ to 27$^{th}$ and November 14$^{th}$ to 17$^{th}$, 2014. Both episodes showed accumulation of ozone and $PM_{2.5}$. The total OH reactivity level also built up significantly (Fig 5b).

### 3.3 Variations in missing reactivity

Significant differences were found between the measured reactivity and calculated reactivity which derived from mixing ratios of different species multiplied by their rate coefficients with OH radicals, as presented in Fig 5a for Beijing and Fig 5b for Heshan. Taking all measured species into consideration, $NO_x$ and NMHCs showed the largest contribution, 45%-55% of total OH reactivity (Fig 9). The OVOCs had also significant contribution, and measured OVOCs had a sharing of 10% in total reactivity in Beijing while 7% in Heshan.

The Missing reactivity was on average over 4 $s^{-1}$, 21 ± 17 % of the total OH reactivity in Beijing and 10 $s^{-1}$, 32 ± 21% in Heshan. The missing reactivity presented different temporal patterns. In Beijing, the missing reactivities were high during pollution episodes, especially in the morning rush hours. The percentage of missing reactivity could reach over 50%. For the Heshan site, the missing reactivity was more or less stable during the entire campaign. Even in clean days with reactivity levels lower than 20 $s^{-1}$, 20%-30% of missing reactivity still existed.

# 4. Discussion

## 4.1 Reactivity levels in Beijing and Heshan

The measured VOCs reactivity (obtained by subtracting inorganic reactivity from total OH reactivity), 11.2 $s^{-1}$ in Beijing and 18.3 $s^{-1}$ in Heshan (Fig 10), was actually not at high end comparing with the levels from literatures. Tokyo presented a similar level of VOCs reactivity (Yoshino et al., 2006). The measured NMHCs levels (obtained by adding all hydrocarbon mixing ratios together) were also not very high, with Beijing 2013 being around 20 ppbV and Heshan 2014 higher than 35 ppbV. The relative VOCs reactivity, defined by the ratio of the VOCs reactivity to the measured NMHCs levels, the values for both Beijing and Heshan were very high.

One possible explanation is the higher content of reactive hydrocarbons in China. Compared to other campaigns, both sites had higher loading of alkenes and aromatics (Yuan et al., 2012; Wang et al., 2014b). The other probable reason is the contribution from OVOCs. In Beijing and Heshan, ambient formaldehyde could accumulate to over 10 ppbV, which was significantly higher than levels found in other observations

(Li et al., 2013; Chen et al., 2014). Another possible explanation is unmeasured species, either primary hydrocarbons or secondary products, which will be discussed in later sessions.

### 4.2 Contributions to the missing reactivity: primary VOCs

As missing reactivity was observed at Beijing and Heshan site, the species possibly causing these missing were examined. Throughout the whole campaign at the PKU site, missing reactivity was normally found in the morning, as for an example in August 16$^{th}$ and 17$^{th}$ 2013 in (Fig 11). Between 5 a.m. to 10 a.m., local vehicle-related sources were strong, and the chemical reactions were not active yet, and the oxidants levels thus the secondary VOC species remained low. We assumed that the unmeasured primary VOCs species could most likely be the major contributors to missing reactivity. Special attention was paid to the unmeasured branched-alkenes for their high reactivity and was previously observed from vehicle exhaust (Nakashima et al., 2010) and gasoline evaporation emissions (Wu et al., 2015). We found only one dataset of branched alkenes measurements in Beijing, 2005 measured by NOAA (Liu et al., 2009). We chose the diurnal patterns of missing reactivity in Beijing in 2013 and compared to the diel cycles of four measured branched-alkenes in 2005. The correlations were found as presented in Fig 11. Considering the contribution of the 4 branched alkenes, the VOCs reactivity could be enhanced by 2.3 $s^{-1}$. This could only partially explain the missing VOCs reactivity which was around 10 $s^{-1}$. With observed decreasing trends in mixing ratios of most NMHCs species in Beijing (Zhang et al., 2014; Wang et al., 2015), the branched-alkenes were insufficient to tell the full story of the missing reactivity. Unmeasured semi-volatile organic compounds (SVOCs) and intermediate volatile organic compounds (IVOCs), such as alkanes between C12 to C30, and polycyclic aromatic hydrocarbons (PAHs) could be also important. Sheehy (2010) found SVOCs and IVOCs contributed to about 10% in morning time in Mexico City. Future studies with a wider range of reactive VOCs measurement for total OH reactivity closure is needed.

### 4.3 Contributions to the missing reactivity: secondary VOCs

Due to limitations in chemistry mechanisms as well as measuring techniques,

418 secondary products are not fully quantified in ambient air and could probably
419 contribute significantly to the observed missing reactivity, especially in the urban or
420 suburban sites receiving chemically complex aged air masses.

421 Besides the large missing reactivity during the morning rush hour, there was
422 about 25% difference between measured and calculated reactivity from August 16$^{th}$ to
423 18$^{th}$, 2013 at PKU site. Considering high levels of oxidants in daytime, the mixing
424 ratios of branched-alkenes could be lower than 0.1 ppbV, which could not explain the
425 observed missing reactivity. A box model was deployed to investigate the role of
426 secondary species in variation of VOCs reactivity. The model, constrained by
427 measured parameters (meteorology, inorganic gases, VOCs including measured
428 carbonyls), gave the results of VOCs reactivity which agreed well with the measured
429 reactivity in most of the daytime (Fig 11). Major contributors from modeled species
430 were unmeasured aldehydes, glyoxal and methyl glyoxal. Average values of major
431 secondary contributors to modelled reactivity were provided in Table S5. However,
432 the missing in morning hours remain unsolved: In the model run, the higher secondary
433 contribution on August 17$^{th}$ 2013 morning was owing to isoprene oxidation products,
434 by using 1.5 ppbv of isoprene levels as model input, the missing reactivity kept over
435 40% around 7:00 and 8:00 a. m.

436 The similar model was applied for the Heshan observation (Fig 12). During the
437 polluted episode between October 24$^{th}$ and 27$^{th}$ 2014, a 30% missing reactivity existed
438 for most time. Unfortunately, the modeled reactivity was only 10-20% higher than
439 calculated reactivity, and not enough to explain the measured reactivity. The major
440 contributors among modeled species were also unmeasured aldehydes, glyoxal,
441 methyl glyoxal and other secondary products, as shown in Table S6. Due to strong
442 emissions of aromatics from solvent use and petroleum industry in PRD region
443 (Zheng et al., 2009), high levels of glyoxal and methyl glyoxal in this region were
444 observed from satellite measurement (Liu et al., 2012) and ground measurements (Li
445 et al., 2013). Compared to the 2006 measurements in Back garden, a semi-rural site in
446 PRD region, the modeled glyoxal was twice as high as around 0.8 ppbV (Li et al.,
447 2013). This difference possibly resulted from higher levels of precursors in 2014

448 measurements, where the measured reactivity was about 50% higher than the results
449 in Backgarden 2006 (Lou et al., 2010).

450 **4.4 Implications for ozone production efficiency**

451 The investigating of missing in VOCs reactivity is expected to better understand
452 the ozone formation processes. To evaluate this contribution, we employed the box
453 model to calculate the influence of VOCs reactivity on OPE. We set two scenarios for
454 the model run: 1) The base run was constrained with measured species, including all
455 inorganic compounds, PAMS 56 hydrocarbons, TO-15 OVOCs and formaldehyde.
456 This is how we obtained the modelled reactivity as presented above, and the
457 intermediates and oxidation products were reproduced as well. 2) The other scenario
458 used measured reactivity as a constraint. Due to the difference between measured and
459 modeled reactivity, we allocated the missing reactivity into several groups. For the
460 primary species, we assumed the ratio between total chain-alkenes and
461 branched-alkenes were the same in Beijing 2013 and in Heshan 2014 as the ratio in
462 Beijing 2005, so we got the assumed mixing ratios of branched-alkenes at both sites.
463 For secondary species, we allocated the remaining missing reactivity into different
464 intermediates or products based on weights obtained in the model base run. Under
465 both assumptions, we ran the OBM and calculated the OPE, as presented in Fig 13.

466 For both sites, the OPE constrained by measured reactivity were significantly
467 higher than the OPE we calculated from modeled reactivity. In Beijing, the OPE from
468 measured reactivity was about 21% higher on average. The value was 30% higher at
469 Heshan site under similar assumptions. This percentage was close to the percentage of
470 missing reactivity, indicating the ignorance of unmeasured or unknown organic
471 species can cause significant underestimation in ozone production calculation. When
472 the four branched-alkenes were included in the OPE calculation, the OPE results
473 would be 4% higher than the OPE constrained by calculated reactivity, but still far
474 from the OPE constrained by measured reactivity.

475 Compared to other similar calculations worldwide, the OPE results for Beijing
476 and Heshan were significantly higher (Fig 14). The comparison was made for $NO_x$ =
477 20 ppbV which was in the range of most observation results. For urban measurements,

478 only the results from Mexico City in MCMA-03 were close to the Beijing results in
479 basic model run (Lei et al., 2008). For suburban measurements, the OPE in Heshan
480 2014 was higher than all other three campaigns, even including the results from
481 Shangdianzi station in CAREBEIJING-2008 campaigns (Ge et al., 2012). While
482 taking missing reactivity into consideration, the OPE results were even higher,
483 indicating more ozone was produced by the reactions of the same quantity of $NO_x$
484 molecules.

485 ## 5. Conclusions

486 In this study, total OH reactivity measurements employing CRM system were
487 conducted at PKU site in Beijing 2013, and Heshan site 2014 in PRD region.
488 Comparisons between measured and calculated, as well as modelled reactivity were
489 made and possible reasons for the missing reactivity have been investigated. The
490 contribution of missing reactivity to ozone production efficiency was evaluated.

491 In Beijing 2013, daily median result for measured total OH reactivity was 20 ±
492 11 $s^{-1}$. Similar diurnal variation with other urban measurements was found with peaks
493 over 25 $s^{-1}$ during the morning rush hour and lower reactivity than 16 $s^{-1}$ in the
494 afternoon. In Heshan 2014, total OH reactivity was 31 ± 20 $s^{-1}$ on daily median result.
495 The diurnal variation was not significant. Both sites have experienced OH reactivity
496 over 80 $s^{-1}$ during polluted episodes.

497 Missing reactivity was found at both sites. While in Beijing the missing
498 reactivity made up 21% of measured reactivity, some periods even reached a higher
499 missing percentage as 40%-50%. In Heshan, missing reactivity's contribution to total
500 OH reactivity was 32% on average and quite stable for the whole day. Unmeasured
501 primary species, such as branched-alkenes could be important contributor to the
502 missing reactivity in Beijing, especially in morning rush hour, but they were not
503 enough to explain Aug 17$^{th}$ morning's event. With the help of RACM2, unmeasured
504 secondary products were calculated and thus the modelled reactivity could agree with
505 measured reactivity in Beijing in the noontime. However, they were still not enough
506 to explain the missing reactivity in Heshan, even in daytime. This was probably

because of the relatively higher oxidation stage in Heshan than in Beijing.

Missing reactivity could impact the estimation of atmospheric ozone production efficiency. Compared to modeled reactivity from base run, ozone production efficiency would rise 21% and 30% in Beijing and Heshan with measured reactivity applied. Both results were significantly higher than similar observations worldwide, indicating the relatively faster ozone production at both sites.

However, in order to further explore the OH reactivity in both regions, more efforts should be paid in both OH reactivity measurements and speciated measurements, as well as modeling to close the total OH reactivity budget. Moreover, a thorough way with more detailed mechanisms should be established to connect the missing reactivity to the evaluation of ozone production.

## Acknowledgement

This study was funded by the National Key Research and Development Plan (grant no. 2016YFC020200), Natural Science Foundation for Outstanding Young Scholars (grant no. 41125018) and a Natural Science Foundation key project (grant no.411330635). The research was also supported by the European Commission Partnership with China on Space Data (PANDA project). Special thanks to Jing Zheng, Mei Li, Yuhan Liu from Peking University and Tao Zhang from Guangdong Environmental Monitoring Center for the help, thanks for William. C. Kuster from NOAA . Earth System Research Laboratory for the branched-alkenes data in 2005.

# Reference


Barletta, B., Meinardi, S., Sherwood Rowland, F., Chan, C.-Y., Wang, X., Zou, S., Yin Chan, L., and Blake, D. R.: Volatile organic compounds in 43 Chinese cities, Atmos. Environ., 39, 5979-5990, doi: 10.1016/j.atmosenv.2005.06.029, 2005.

Calpini, B., Jeanneret, F., Bourqui, M., Clappier, A., Vajtai, R., and van den Bergh, H.: Direct measurement of the total reaction rate of OH in the atmosphere, Analusis, 27, 328-336, doi: 10.1051/analusis:1999270328, 1999.

Chatani, S., Shimo, N., Matsunaga, S., Kajii, Y., Kato, S., Nakashima, Y., Miyazaki, K., Ishii, K., and H., U.: Sensitivity analyses of OH missing sinks over Tokyo metropolitan area in the summer of 2007, Atmos. Chem. Phys., 9, 8975-8986, doi: 10.5194/acp-9-8975-2009, 2009.

Chen, W. T., Shao, M., Lu, S. H., Wang, M., Zeng, L. M., Yuan, B., Liu, Y.: Understanding primary and secondary sources of ambient carbonyl compounds in Beijing using the PMF model. Atmos. Chem. Phys., 14, 3047-3062, doi: 10.5194/acp-14-3047-2014, 2014.

Chou, C. C. K., Tsai, C. Y., Chang, C. C., Lin, P. H., Liu, S. C., and Zhu, T.: Photochemical production of ozone in Beijing during the 2008 Olympic Games, Atmos. Chem. Phys., 11, 9825-9837, doi: 10.5194/acp-11-9825-2011, 2011.

Dodge, M. C.: Proceedings of the international conference on photochemical oxidant pollution and its control. Combined use of modeling techniques and smog chamber data to derive ozone-precursor relationships, U.S. Environmental Protection Agency, Research Triangle Park, NC, 881-889 pp., 1977.

de Gouw, J. A., Middlebrook, A. M., Warneke, C., Goldan, P. D., Kuster, W. C., Roberts, J. M., Fehsenfeld, F. C., Worsnop, D. R., Canagaratna, M. R., Pszenny, A. A. P., Keene, W. C., Marchewka, M., Bertman, S. B., Bates, T. S.: Budget of organic carbon in a polluted atmosphere: Results from the New England Air Quality Study in 2002, J. Geophy. Res.-Atmos., 110, D16305, doi: 10.1029/2004jd005623, 2005.

Dolgorouky, C., Gros, V., Sarda-Esteve, R., Sinha, V., Williams, J., Marchand, N., Sauvage, S., Poulain, L., Sciare, J., and Bonsang, B.: Total OH reactivity measurements in Paris during the 2010 MEGAPOLI winter campaign, Atmos. Chem. Phys., 12, 9593-9612, doi: 10.5194/acp-12-9593-2012, 2012.

Edwards, P. M., Evans, M. J., Furneaux, K. L., Hopkins, J., Ingham, T., Jones, C., Lee, J. D., Lewis, A. C., Moller, S. J., Stone, D., Whalley, L. K., and Heard, D. E.: OH

570 reactivity in a South East Asian tropical rainforest during the Oxidant and Particle
571 Photochemical Processes (OP3) project, Atmos. Chem. Phys., 13, 9497-9514, doi:
572 10.5194/acp-13-9497-2013, 2013.
573 Fang, X., Shao, M., Stohl, A., Zhang, Q., Zheng, J., Guo, H., Wang, C., Wang, M., Ou,
574 J., Thompson, R. L., and Prinn, R. G.: Top-down estimates of benzene and toluene
575 emissions in the Pearl River Delta and Hong Kong, China, Atmos. Chem. Phys., 16,
576 3369-3382, doi: 10.5194/acp-16-3369-2016, 2016.
577 Fuchs, H., Hofzumahaus, A., Rohrer, F., Bohn, B., Brauers, T., Dorn, H. P., Häseler,
578 R., Holland, F., Kaminski, M., Li, X., Lu, K., Nehr, S., Tillmann, R., Wegener, R., and
579 Wahner, A.: Experimental evidence for efficient hydroxyl radical regeneration in
580 isoprene oxidation, Nature Geoscience, 6, 1023-1026, doi: 10.1038/ngeo1964, 2013.
581 Fuchs, H., Tan, Z. F., Lu, K. D., Bohn, B., Broch, B., Brown, S. S., Dong, H. B.,
582 Gomm. S., Haseler, H. L. Y., Hofzumahaus, A., Holland, F., Li, X., Liu, Y., Lu, S. H.,
583 Min, K.-E., Rohrer, F., Shao, M., Wang, B. L., Wang, M., Wu, Y. S., Zeng, L. M.,
584 Zhang, Y. S., Wahner, A., Zhang, Y. H.: OH reactivity at a rural site (Wangdu) in the
585 North China Plain: Contributions from OH reactants and experimental OH budget,
586 Atmos. Chem. Phys., Dis., 716-745, doi: 10.5194/acp-2016-716, 2016.
587 Ge. B. Z., Sun. Y. L., Liu. Y., Dong. H. B., Ji. D. S., Jiang. Q., Li. J., Wang. Z. F.:
588 Nitrogen dioxide measurement by cavity attenuated phase shift spectroscopy (CAPS)
589 and implications in ozone production efficiency and nitrate formation in Beijing,
590 China. J. Geophy. Res.-Atmos., 118, 9499-9509, doi: 10.1002/jgrd.50757, 2013.
591 Geddes, J. A., Murphy, J. G., and K., W. D.: Long term changes in nitrogen oxides and
592 volatile organic compounds in Toronto and the challenges facing local ozone control,
593 Atmos. Environ., 43, 3407-3415, doi: 10.1016/j.atmosenv.2009.03.053, 2009.
594 Geiger, H., Barnes, I., Bejan, I., Benter, T., and Spittler, M.: The tropospheric
595 degradation of isoprene: an updated module for the regional atmospheric chemistry
596 mechanism, Atmos. Environ., 37, 1503–1519, doi: 10.1016/S1352-2310(02)01047-6,
597 2003.
598 Goliff, W. S., Stockwell, W. R., Lawson, C. V.: The regional atmospheric chemistry
599 mechanism, version 2. Atmos. Environ., 68, 174-185, doi: 10.1016/j.atmosenv.2012.
600 11.038, 2013
601 Guo, J. P., Miao, Y. C., Zhang, Y., Liu, H., Li, Z. Q., Zhang, W. C. He, J., Lou, M. Y.,
602 Yan, Y., Bian, L. G., Zhai, P. M.: The climatology of planetary boundary layer height
603 in China derived from radiosonde and reanalysis data., Atmos. Chem. Phys., 16,

13309-13319, doi: 10.5194/acp-16-13309-2016, 2016

Hansen, R. F., Blocquet, M., Schoemaecker, C., Léonardis, T., Locoge, N., Fittschen, C., Hanoune, B., Stevens, P. S., Sinha, V., and Dusanter, S.: Intercomparison of the comparative reactivity method (CRM) and pump–probe technique for measuring total OH reactivity in an urban environment, Atmos. Meas. Tech., 8, 4243-4264, doi: 10.5194/amt-8-4243-2015, 2015.

Ingham, T., Goddard, A., Whalley, L. K., Furneaux, K. L., Edwards, P. M., Seals, C. P., Self, D. E., Johnson, G. P., Read, K. A., Lee, J. D., and E., H. D.: a flow tube based LIF instrument to measure OH reactivity in the troposphere, Atmos. Meas. Tech., 2, 465-477, doi: 10.5194/amt-2-465-2009, 2009.

Karl, M., Dorn, H.-P., Holland, F., Koppmann, R., Poppe, D., Rupp, L., Schaub, A., and Wahner, A.: Product study of the reaction of OH radicals with isoprene in the atmosphere simulation chamber SAPHIR, J. Atmos. Chem., 55, 167–187, doi: 10.1007/s10874-006-9034-x, 2006.

Kato, S, Sato, T., Kaji, Y.: A method to estimate the contribution of unidentified VOCs to OH reactivity. Atmos. Environ., 45, 5531-5539, doi: 10.1016/j.atmosenv.2011.05. 074. 2011.

Kleinman, L. I., Daum, P. H., Imre, D. G., Lee. J. H., Lee. Y. N., Nunnermacker, L. J., Springston, S. R., Weinstein-Lloyd, J., Newman, L.: Ozone production in the New York City urban plume. J. Geophy. Res.-Atmos., 105, D11, 14495-14511, doi: 10.1029/2000 jd900011, 2000.

Kleinman, L. I.: Ozone production efficiency in an urban area, J. Geophy. Res. – atmos., 107, D23, 4733, doi: 10.1029/2002jd002529, 2002.

Kovacs, T. A., and Brune, W. H.: Total OH loss rate measurement, J. Atmos. Chem., 39, 105-122, doi: 10.1023/a:1010614113786, 2001.

Kovacs, T. A., Brune, W. H., Harder, H., Martinez, M., Simpas, J. B., Frost, G. J., Williams, A. G., Jobson, B. T., Stroud, C., Young, V., Fried, A., and B., W.: Direct measurements of urban OH reactivity during Nashville SOS in summer 1999, J. Environ. Monit., 5, 68-74, doi: 10.1039/b204339d, 2003.

Kumar V., Sinha, V.: VOC-OHM: a new technique for rapid measurements of ambient total OH reactivity and volatile organic compounds using a single proton transfer reaction mass spectrometer. Int. J. of Mass Spectrom., 374, 55-63. 2014.

LaFranchi, B. W., Goldstein, A. H., and Cohen, R. C.: Observations of the temperature dependent response of ozone to $NO_x$ reductions in the Sacramento, CA

638 urban plume, Atmos. Chem. Phys., 11, 6945-6960, doi: 10.5194/acp-11-6945-2011,
639 2011.
640 Lee, J. D., Young, J. C., Read, K. A., Hamilton, J. F., Hopkins, J. R., Lewis, A. C.,
641 Bandy, B. J., Davey, J., Edwards, P. M., Ingham, T., Self, D. E., Smith, S. C., Pilling,
642 M. J., and Heard, D. E.: Measurement and calculation of OH reactivity at a United
643 Kingdom coastal site, J. Atmos. Chem., 64, 53-76, doi: 10.1007/s10874-010-9171-0,
644 2010.
645 Lei, W., Zavala, M., Foy, B. de., Volkamer, R., Molina, L. T.: Characterizing ozone
646 production and response under different meteorological conditions in Mexico City.
647 Atmos. Chem. Phys., 8, 7571-7581, doi: 10.5194/acp-8-7571-2008, 2008.
648 Li, M., Shao, M., Li, L.-Y., Lu, S.-H., Chen, W.-T., and Wang, C.: Quantifying the
649 ambient formaldehyde sources utilizing tracers, Chinese. Chem. Lett., 25, 1489-1491,
650 doi: 10.1016/j.cclet.2014.07.001, 2014.
651 Li, X., Brauers, T., Hofzumahaus, A., Lu, K., Li, Y. P., Shao, M., Wagner, T., and
652 Wahner, A.: MAX-DOAS measurements of $NO_2$, HCHO and CHOCHO at a rural site
653 in Southern China, Atmos. Chem. Phys., 13, 2133-2151, doi:
654 10.5194/acp-13-2133-2013, 2013.
655 Liu, Y., Shao, M., Fu, L., Lu, S., Zeng, L., and Tang, D.: Source profiles of volatile
656 organic compounds (VOCs) measured in China: Part I, Atmos. Environ., 42,
657 6247-6260, doi: 10.1016/j.atmosenv.2008.01.070, 2008.
658 Liu, Y., Shao, M., Kuster, W. C., Goldan, P. D., Li, X. H., Lu, S. H., de Gouw, J. A.:
659 Source identification of reactive hydrocarbons and oxygenated VOCs in the
660 summertime in Beijing. Environ. Sci. Technol., 43, 75-81, doi: 10.1021/es801716n,
661 2009.
662 Liu, Y. H., Lu, K. D., Dong, H. B., Li, X., Cheng, P., Zou, Q., Wu, Y. S., Liu, X. G.,
663 Zhang, Y. H. In situ monitoring of atmospheric nitrous acid based on multi-pumping
664 flow system and liquid waveguide capillary cell. J. Envion. Sci. Accepted. 2016.
665 Liu, Z., Wang, Y., Vrekoussis, M., Richter, A., Wittrock, F., Burrows, J. P., Shao, M.,
666 Chang, C.-C., Liu, S.-C., Wang, H., and Chen, C.: Exploring the missing source of
667 glyoxal (CHOCHO) over China, Geophy. Res. Lett., 39, L10812, doi:
668 10.1029/2012gl051645, 2012.
669 Lou, S., Holland, F., Rohrer, F., Lu, K., Bohn, B., Brauers, T., Chang, C. C., Fuchs, H.,
670 Häseler, R., Kita, K., Kondo, Y., Li, X., Shao, M., Zeng, L., Wahner, A., Zhang, Y.,
671 Wang, W., and Hofzumahaus, A.: Atmospheric OH reactivities in the Pearl River

672 Delta – China in summer 2006: measurement and model results, Atmos. Chem. Phys.,
673 10, 11243-11260, doi: 10.5194/acp-10-11243-2010, 2010.
674 Lu, K. D., Zhang, Y. H., Su, H., Brauers, T., Chou, C. C., Hofzumahaus, A., Liu, S. C.,
675 Kita, K., Kondo, Y., Shao, M., Wahner, A., Wang, J. L., Wang, X., and T., Z.: Oxidant
676 ($O_3$+ $NO_2$) production processes and formation regimes in Beijing, J. Geophys.
677 Res.-Atmos., 115, D07303, doi: 10.1029/2009jd012714, 2010.
678 Lu, K. D., Hofzumahaus, A., Holland, F., Bohn, B., Brauers, T., Fuchs, H., Hu, M.,
679 Häseler, R., Kita, K., Kondo, Y., Li, X., Lou, S. R., Oebel, A., Shao, M., Zeng, L. M.,
680 Wahner, A., Zhu, T., Zhang, Y. H., and Rohrer, F.: Missing OH source in a suburban
681 environment near Beijing: observed and modelled OH and $HO_2$ concentrations in
682 summer 2006, Atmos. Chem. Phys., 13, 1057-1080, doi: 10.5194/acp-13-1057-2013,
683 2013.
684 Mao, J. Q., Ren, X. R., Chen, S., Brune, W. H., Chen, Z., Martinez, M., Harder, H.,
685 Lefer, B., Rappengluck, B., Flynn, J., and M., L.: Atmospheric oxidation capacity in
686 the summer of Houston 2006: Comparison with summer measurements in other
687 metropolitan studies, Atmos. Environ., 44, 4107-4115, doi: 10.1016/j.atmosenv.2009.
688 01.013, 2010.
689 Michoud, V., Hansen, R. F., Locoge, N., Stevens, P. S., and Dusanter, S.: Detailed
690 characterizations of the new Mines Douai comparative reactivity method instrument
691 via laboratory experiments and modeling, Atmos. Meas. Tech., 8, 3537-3553, doi:
692 10.5194/amt-8-3537-2015, 2015.
693 Nölscher, A. C., Williams, J., Sinha, V., Custer, T., Song, W., Johnson, A. M., Axinte,
694 R., Bozem, H., Fischer, H., Pouvesle, N., Phillips, G., Crowley, J. N., Rantala, P.,
695 Rinne, J., Kulmala, M., Gonzales, D., Valverde-Canossa, J., Vogel, A., Hoffmann, T.,
696 Ouwersloot, H. G., Vilà-Guerau de Arellano, J., and Lelieveld, J.: Summertime total
697 OH reactivity measurements from boreal forest during HUMPPA-COPEC 2010,
698 Atmos. Chem. Phys., 12, 8257-8270, doi: 10.5194/acp-12-8257-2012, 2012.
699 Nölscher, A. C., Yanez-Serrano, A. M., Wolff, S., de Araujo, A. C., Lavric, J. V.,
700 Kesselmeier, J., and Williams, J.: Unexpected seasonality in quantity and composition
701 of Amazon rainforest air reactivity, Nature communications, 7, 10383-10394, doi:
702 10.1038/ncomms10383, 2016.
703 Nakashima, Y., Kamei, N., Kobayashi, S., and Y., K.: Total OH reactivity and VOC
704 analyses for gasoline vehicular exhaust with a chassis dynamometer, Atmos. Environ.,
705 44, 468-475, doi: 10.1016/j.atmosenv.2009.11.006, 2010.

706 Pöschl, U., von Kuhlmann, R., Poisson, N., and Crutzen, P. J.: Development and
707 intercomparison of condensed isoprene oxidation mechanisms for global atmospheric
708 modeling, J. Atmos. Chem., 37, 29–52, doi: 10.1023/A:1006391009798, 2000.
709 Ren, X. R., Harder, H., Martinez, M., Lesher, R. L., Oliger, A., Shirley, T., Adams, J.,
710 Simpas, J. B., and H., B. W.: $HO_x$ concentrations and OH reactivity observations in
711 New York City during PMTACS-NY2001, Atmos. Environ., 37, 3627-3637, doi:
712 10.1016/s1352-2310(03)00460-6, 2003.
713 Ren, X. R., Brune, W. H., Cantrell, C., Edwards, G. D., Shirley, T., Metcalf, A. R., and
714 L., L. R.: Hydroxyl and Peroxy Radical Chemistry in a Rural Area of Central
715 Pennsylvania: Observations and Model Comparisons, J. Atmos. Chem., 52, 231-257,
716 doi: 10.1007/s10874-005-3651-7, 2005.
717 Ren, X. R., Brune, W. H., Mao, J. Q., Mitchell, M. J., Lesher, R. L., Simpas, J. B.,
718 Metcalf, A. R., Schwab, J. J., Cai, C., and Y., L.: Behavior of OH and $HO_2$ in the
719 winter atmosphere in New York City, Atmos. Environ. 40, 252-263, doi:
720 10.1016/j.atmosenv. 2005.11.073, 2006a.
721 Ren, X. R., Brune, W. H., Oliger, A., Metcalf, A. R., Simpas, J. B., Shirley, T.,
722 Schwab, J. J., Bai, C., Roychowdhury, U., Li, Y., Cai, C., Demerjian, K. L., He, Y.,
723 Zhou, X. H., Gao, H., and J., H.: OH, $HO_2$, and OH reactivity during the
724 PMTACS–NY Whiteface Mountain 2002 campaign: Observations and model
725 comparison, J. Geophys. Res.-Atmos., 111, doi: 10.1029/2005jd006126, 2006b.
726 Sadanaga, Y., Yoshino, A., Kato, S., Yoshioka, A., Watanabe, K., Miyakawa, T.,
727 Hayashi, I., Ichikawa, M., Matsumoto, J., Nishiyama, A., Akiyama, N., Kanaya, Y.,
728 and Y., K.: The importance of $NO_2$ and volatile organic compounds in the urban air
729 from the viewpoint of the OH reactivity, Geophy. Res. Lett., 31, L08102, doi:
730 10.1029/2004gl019661, 2004.
731 Sadanaga, Y., Yoshino, A., Kato, S., and Y., K.: measurements of OH reactivity and
732 photochemical ozone production in the urban atmosphre, Environ. Sci. Technol., 39,
733 8847-8852, doi: 10.1021/es049457p, 2005.
734 Sheehy, P. M., Volkamer, R., Molina, L. T., and Molina, M. J.: Oxidative capacity of
735 the Mexico City atmosphere – Part 2: A $RO_x$ radical cycling perspective, Atmos.
736 Chem. Phys., 10, 6993-7008, doi: 10.5194/acp-10-6993-2010, 2010.
737 Shirley, T. R., Brune, W. H., Ren, X. R., Mao, J. Q., Lesher, R., Cardenas, B.,
738 Volkamer, R., Molina, L. T., Molina, M. J., Lamb, B., Velasco, E., Jobson, T., and M.,
739 A.: Atmospheric oxidation in the MCMA during April 2003, Atmos. Chem. Phys., 6,

2753-2765, doi: 10.5194/acp-6-2753-2006, 2006.
Sinha, V., Williams, J., Crowley, J. N., and J., L.: The Comparative Reactivity Method - a new tool to measure total OH reactivity in ambient air, Atmos. Chem. Phys., 8, 2213-2227, doi: 10.5194/acp-8-2213-2008, 2008.
Sinha, V., Custer, T. G., Kluepfel, T., and Williams, J.: The effect of relative humidity on the detection of pyrrole by PTR-MS for OH reactivity measurements, Int. J. Mass Spectrom., 282, 108-111, doi: 10.1016/j.ijms.2009.02.019, 2009.
Sinha, V., Williams, J., Lelieveld, J., Ruuskanen, T. M., Kalos, M. K., Patokoski, L., Hellen, H., Hakola, H., Mogensen, D., Boy, M., Rinne, L., and M., K.: OH reactivity measurements within a boreal forest - evidence for unknown reactive emissions, Environ. Sci. Technol., 44, 6614-6620, doi: 10.1021/es101780b, 2010.
Sinha, V., Williams, J., Diesch, J. M., Drewnick, F., Martinez, M., Harder, H., Regelin, E., Kubistin, D., Bozem, H., Hosaynali-Beygi, Z., Fischer, H., Andrés-Hernández, M. D., Kartal, D., Adame, J. A., and Lelieveld, J.: Constraints on instantaneous ozone production rates and regimes during DOMINO derived using in-situ OH reactivity measurements, Atmos. Chem. Phys., 12, 7269-7283, doi: 10.5194/acp-12-7269-2012, 2012.
Stockwell, W. R., Kirchner, F., Kuhn, M., and Seefeld, S.: A new mechanism for regional atmospheric chemistry modeling, J. Geophys. Res.-Atmos., 102, D22, 25847-25879, doi: 10.1029/97jd00849, 1997.
Stone, D., Whalley, L. K., and Heard, D. E.: Tropospheric OH and $HO_2$ radicals: field measurements and model comparisons, Chem. Soc. Rev., 41, 6348-6404, doi: 10.1039/c2cs35140d, 2012.
Tan, Z. F., Fuchs, H., Zhang, Y. H., et al., Atmos. Chem. Phys., in preparation.
Wang, M., Zeng, L., Lu, S., Shao, M., Liu, X., Yu, X., Chen, W., Yuan, B., Zhang, Q., Hu, M., and Zhang, Z.: Development and validation of a cryogen-free automatic gas chromatograph system (GC-MS/FID) for online measurements of volatile organic compounds, Anal. Methods, 6, 9424-9434, doi: 10.1039/c4ay01855a, 2014a.
Wang, M., Shao, M., Chen, W. T., Yuan, B., Lu, S. H., Zhang, Q., Zeng, L. M., Wang, Q.: A temporally and spatially resolved validation of emission inventories by measurements of ambient volatile organic compounds in Beijing, China. Atmos. Chem. Phys. 14, 5871-5891, doi: 10.5194/acp-14-5871-2014, 2014b.
Wang, M., Shao, M., Chen, W., Lu, S., Liu, Y., Yuan, B., Zhang, Q., Zhang, Q., Chang, C. C., Wang, B., Zeng, L., Hu, M., Yang, Y., and Li, Y.: Trends of non-methane

774 hydrocarbons (NMHC) emissions in Beijing during 2002–2013, Atmos. Chem. Phys.,
775 15, 1489-1502, doi: 10.5194/acp-15-1489-2015, 2015.
776 Wang, T., Ding, A., Gao, J., and Wu, W. S.: Strong ozone production in urban plumes
777 from Beijing, China. Geophy. Res. Lett., 33, L21806, doi: 10.1029/2006gl027689,
778 2006.
779 Whalley, L. K., Stone, D., Bandy, B., Dunmore, R., Hamilton, J. F., Hopkins, J., Lee, J.
780 D., Lewis, A. C., and Heard, D. E.: Atmospheric OH reactivity in central London:
781 observations, model predictions and estimates of in situ ozone production, Atmos.
782 Chem. Phys., 16, 2109-2122, doi: 10.5194/acp-16-2109-2016, 2016.
783 Williams, J.: Provoking the air, Environ. Chem., 5, 317-319, doi:10.1071/en08048,
784 2008.
785 Williams, J., and Brune, W. H.: A roadmap for OH reactivity research, Atmos.
786 Environ., 106, 371-372, doi: 10.1016/j.atmosenv.2015.02.017, 2015.
787 Williams, J., Keßel, S. U., Nölscher, A. C., Yang, Y. D., Lee, Y. N., Yáñez-Serrano, A.
788 M., Wolff, S., Kesselmeier, J., Klüpfel, T., Lelieveld, J., and Shao, M.: Opposite OH
789 reactivity and ozone cycles in the Amazon rainforest and megacity Beijing:
790 Subversion of biospheric oxidant control by anthropogenic emissions, Atmos.
791 Environ., 125, 112-118, doi: 10.1016/j.atmosenv.2015.11.007, 2016.
792 Wu, Y., Yang, Y. D., Shao, M., and Lu, S. H.: Missing in total OH reactivity of VOCs
793 from gasoline evaporation, Chinese. Chem. Lett., 26, 1246-1248, doi:
794 10.1016/j.cclet.2015.05.047, 2015.
795 Yang, Y., Shao, M., Wang, X., Nölscher, A. C., Kessel, S., Guenther, A., and Williams,
796 J.: Towards a quantitative understanding of total OH reactivity: A review, Atmos.
797 Environ.,134, 147-161, doi: 10.1016/j.atmosenv.2016.03.010, 2016.
798 Yoshino, A., Sadanaga, Y., Watanabe, K., Kato, S., Miyakawa, Y., Matsumoto, J., and
799 Y., K.: Measurement of total OH reactivity by laser-induced pump and probe
800 technique—comprehensive observations in the urban atmosphere of Tokyo, Atmos.
801 Environ., 40, 7869-7881, doi: 10.1016/j.atmosenv.2006.07.023, 2006.
802 Yoshino, A., Nakashima, Y., Miyazaki, K., Kato, S., Suthawaree, J., Shimo, N.,
803 Matsunaga, S., Chatani, S., Apel, E., Greenberg, J., Guenther, A., Ueno, H., Sasaki, H.,
804 Hoshi, J., Yokota, H., Ishii, K., and Kajii, Y.: Air quality diagnosis from
805 comprehensive observations of total OH reactivity and reactive trace species in urban
806 central Tokyo, Atmos. Environ., 49, 51-59, doi: 10.1016/j.atmosenv.2011.12.029,
807 2012.

Yuan, B., Shao, M., de Gouw, J., Parrish, D. D., Lu, S., Wang, M., Zeng, L., Zhang, Q., Song, Y., Zhang, J., and Hu, M.: Volatile organic compounds (VOCs) in urban air: How chemistry affects the interpretation of positive matrix factorization (PMF) analysis, J. Geophys. Res.-Atmos., 117, D24302, doi: 10.1029/2012jd018236, 2012.

Zhang, Q., Yuan, B., Shao, M., Wang, X., Lu, S., Lu, K., Wang, M., Chen, L., Chang, C. C., and Liu, S. C.: Variations of ground-level $O_3$ and its precursors in Beijing in summertime between 2005 and 2011, Atmos. Chem. Phys., 14, 6089-6101, doi: 10.5194/acp-14-6089-2014, 2014.

Zhang, Y. H., Su, H., Zhong, L. J., Cheng, Y. F., Zeng, L. M., Wang, X. S., Xiang, Y. R., Wang, J. L., Gao, D. F., and Shao, M.: Regional ozone pollution and observation-based approach for analyzing ozone–precursor relationship during the PRIDE-PRD2004 campaign, Atmos. Environ., 42, 6203-6218, doi: 10.1016/j.atmosenv.2008. 05.002, 2008.

Zhao, C., Wang, Y. H., Zeng, T.,: East China Plains: a "Basin" of ozone pollution, Environ. Sci. Technol., 43, 1911-1915, doi: 10.1021/es8027764, 2009.

Zheng, J. Y., Shao, M., Che, W. W., Zhang, L. J., Zhong, L. J., Zhang, Y. H., Streets, D., Speciated VOC emission inventory and spatial patterns of ozone formation potential in the Pearl River Delta, China. Environ. Sci. Technol. 43, 8580–8586, doi: 10.1021/es901688e, 2009.

Zheng, J. Y., Zhong, L. J., Wang, T., Louie, P. K. K., Li, Z. C.: Ground-level ozone in the Pearl River Delta region: analysis of data from a recently established regional air quality monitoring network. Atmos. Environ. 44, 814-823, doi: 10,1016/j/atmosenv. 2009.11.032, 2010.

Zhao. W., Cohan, D. S., Henderson. B. H.: Slower ozone production in Houston, Texas following emission reductions: evidence from Texas Air Quality Studies in 2000 and 2006. Atmos. Chem. Phys. 14, 2777-2788, doi: 10.5194/acp-14-2777-2014, 2014.

841 Table 1 Total OH reactivity measurements in urban areas

| Campaign | Site | Year | method | $k_{OH(measured)}$ ($s^{-1}$) [a] | $k_{OH\ (calculated)}$ ($s^{-1}$ if it is a value) [b] | Measured species [c] | Reference |
|---|---|---|---|---|---|---|---|
| SOS | Nashville, US | summer, 1999 | LIF-flow tube | 11.3 | 7.2 | SFO | Kovacs et al., 2001; 2003; |
| PMTACS-NY 2001 | NY, US | summer, 2001 | LIF-flow tube | 15~25 | within 10% | SFO | Ren et al., 2003 |
| PMTACS-NY 2004 | NY, US | winter, 2004 | LIF-flow tube | 18-35 | statistically lower | SF | Ren et al., 2006a |
| MCMA-2003 | Mexico City, Mexico | spring, 2003 | LIF-flow tube | 10~120 | 30% less than | -[d] | Shirley et al., 2006 |
| TexAQS | Houston, US | summer, 2000 | LIF-flow tube | 7~12 | agree well | SFO | Mao et al., 2010 |
| TRAMP2006 | Houston, US | summer, 2006 | LIF-flow tube | 9-22 | agree well | SFOB | Mao et al., 2010 |
| | Tokyo, Japan | 2003-2004 | LP-LIF | 10~100 | 30% less than | SFOB | Sadanaga et al., 2004; Yoshino et al., 2006 |
| | Tokyo, Japan | summer, 2006 | LP-LIF | 10~55 | 30% less than | SFOB | Chatani et al., 2009 |
| | Tokyo, Japan | spring, 2009 | LP-LIF | 10~35 | 22% less than | SFOB | Kato et al., 2011 |
| | Tokyo, Japan | winter, 2007, autumn, 2009 | LP-LIF | 10~80 | 10~15 less than | SFOB | Yoshino et al., 2012 |

Table 1 Total OH reactivity measurements in urban areas (continued)

| | | | | | | | |
|---|---|---|---|---|---|---|---|
| | Mainz, German | summer, 2005 | CRM | 10.4 | | - | Sinha et al.,2008 |
| MEGAPOLI | Paris, France | winter, 2010 | CRM | 10~130 | 10~54% less than | SO | Dolgorouky et al., 2012 |
| ClearfLo | London, England | summer, 2012 | LP-LIF | 10-116 | 20~40% | SFOB | Whalley et al., 2016 |
| | Lille, France | autumn , 2012 | CRM, LP-LIF | ~70 | Reasonable agreement | SFO | Hansen et al., 2015 |
| | Dunkirk, France | summer, 2014 | CRM | 10-130 | | - | Michoud et al., 2015 |

a. For sources from different studies, the measured reactivity was presented as the averaged results, or ranges of diurnal variations, or the ranges of the whole campaign.

b. For sources of different studies, the calculated reactivity was presented within an uncertainty range, as a percentage reduction or $s^{-1}$ reduction.

c. Measured species that have been used for the calculated reactivity (following Lou et al., 2010): S = inorganic compounds (CO, $NO_x$, $SO_2$ etc) plus hydrocarbons (including isoprene); F = formaldehyde; O = OVOCs other than formaldehyde; B = BVOCs other than isoprene;

d. "-" means a lack of information regarding what has been measured or how long it has been measured.

853

854 Table2 Total OH reactivity measurements in suburban and surrounding areas

| Campaign | Site | Year | method | $k_{OH(measured)}$ ($s^{-1}$) | $k_{OH\ (calculated)}$ ($s^{-1}$ if it is a value) | Measured Species | Reference |
|---|---|---|---|---|---|---|---|
| | Central Pennsylvania, US | spring, 2002 | LIF-flow tube | 6.1 | | - | Ren et al., 2005 |
| PMTACS-NY2002 | Whiteface Mountain, US | summer, 2002 | LIF-flow tube | 5.6 | within 10% | - | Ren et al., 2006b |
| TORCH-2 | Weybourne, England | spring, 2004 | LIF-flow tube | 4.85 | 2.95 | SFO | Ingham et al., 2009<br>Lee et al., 2010 |
| CareBeijing-2006 | Yufa, China | summer, 2006 | LP-LIF | 10-30 | agree well | S | Lu et al., 2010; 2013 |
| PRIDE-PRD | Backgarden, China | summer, 2006 | LP-LIF | 10~120 | 50% less than | S | Lou et al., 2010 |
| DOMINO | El Arenosillo, Spain | winter, 2008 | CRM | 6.3~85 | | SF | Sinha et al., 2012 |
| | | spring, 2013 | CRM | 53 | 23 | SFOB | Kumar & Sinha., 2014 |

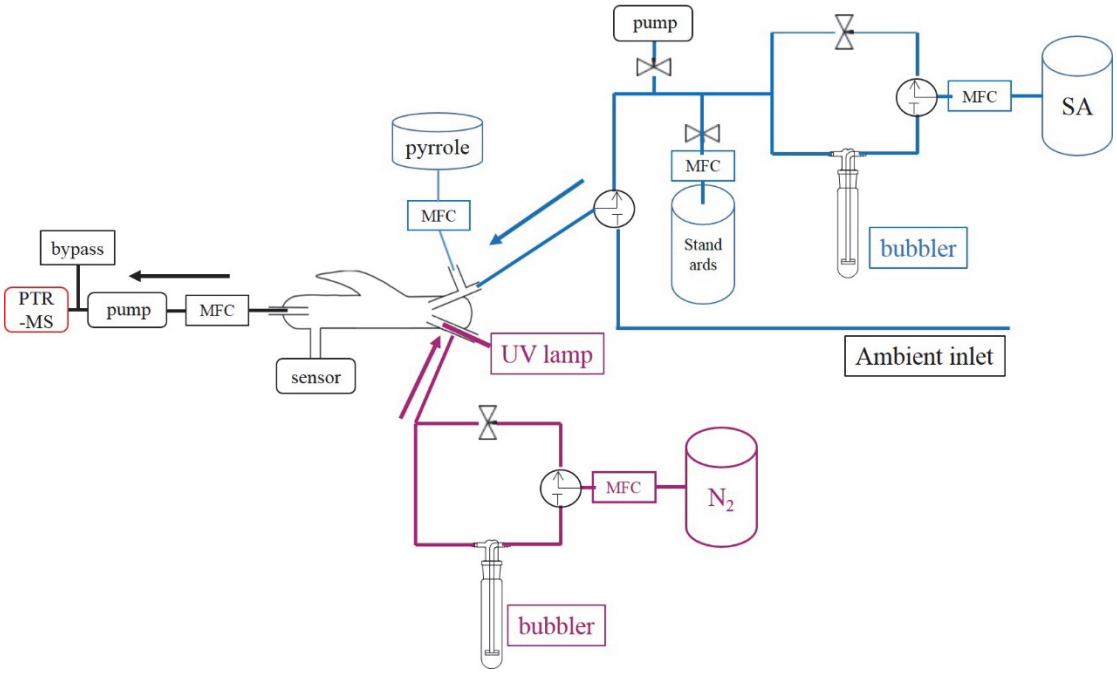


855

856 Fig 1 Schematic figures of CRM system in Beijing and Heshan observations.

857 Blue color represents ambient air or synthetic air injection system, purple color

858 represents OH generating system, black color represents the detection system.

859 Pressure is measured by the sensor connected to the glass reaction.

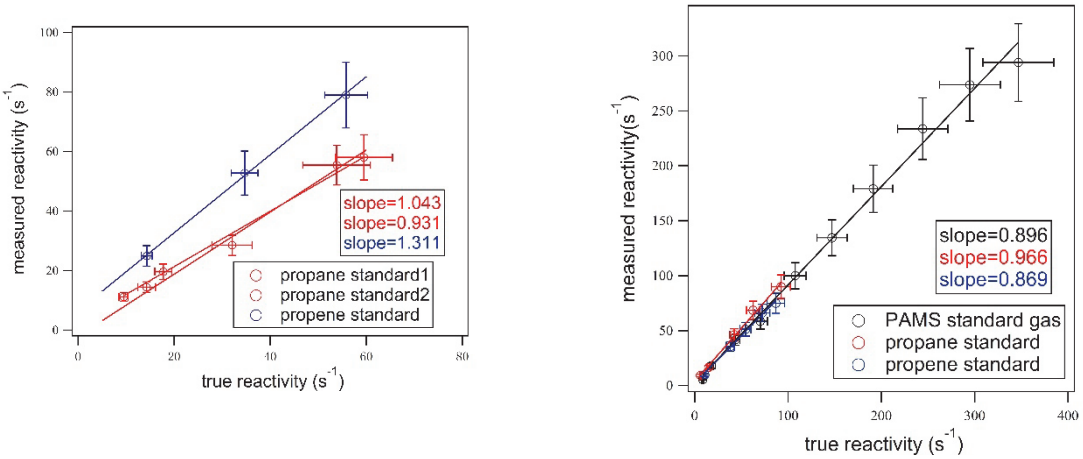


860 Fig 2 OH reactivity calibration in Beijing (left) and Heshan (right).

861 Left: Calibration in Beijing used two single standards: propane, propene;

862 Right: Calibration in Heshan used three standards: propane, propene, mixed PAMS 56

863 NMHCs.

864 Error bars stand for estimated uncertainty on the measured and true reactivity.

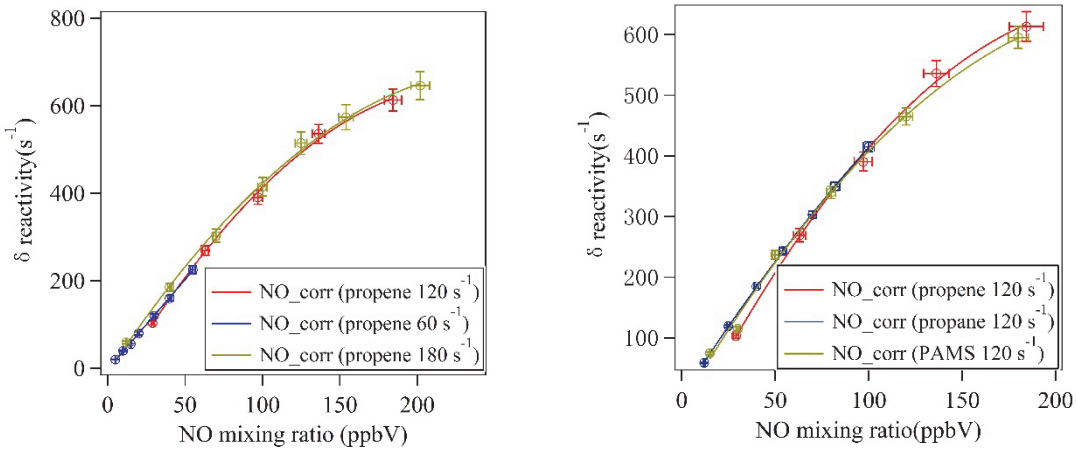


865

866 Fig 3 NO-correction experiments and fitting curves in Heshan 2014.

867 Left: NO-correction experiments with different mixing ratios of propene standard gas;

868 Right: NO-correction experiments with different standard gases at the same reactivity

869 level: 120 $s^{-1}$.

870 Error bars stand for estimated uncertainty on the NO mixing ratios and difference in

871 reactivity.

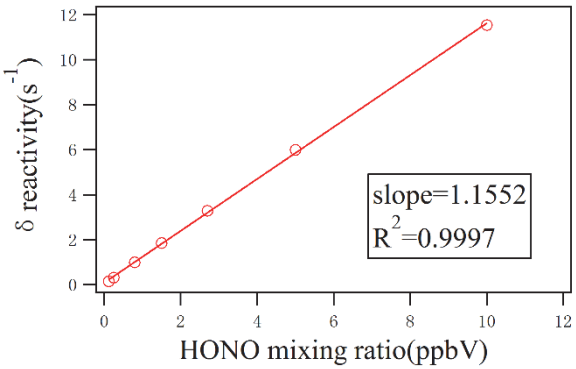


872

873 Fig 4 HONO-correction experiments and the fitting curve in Heshan 2014.

874

875

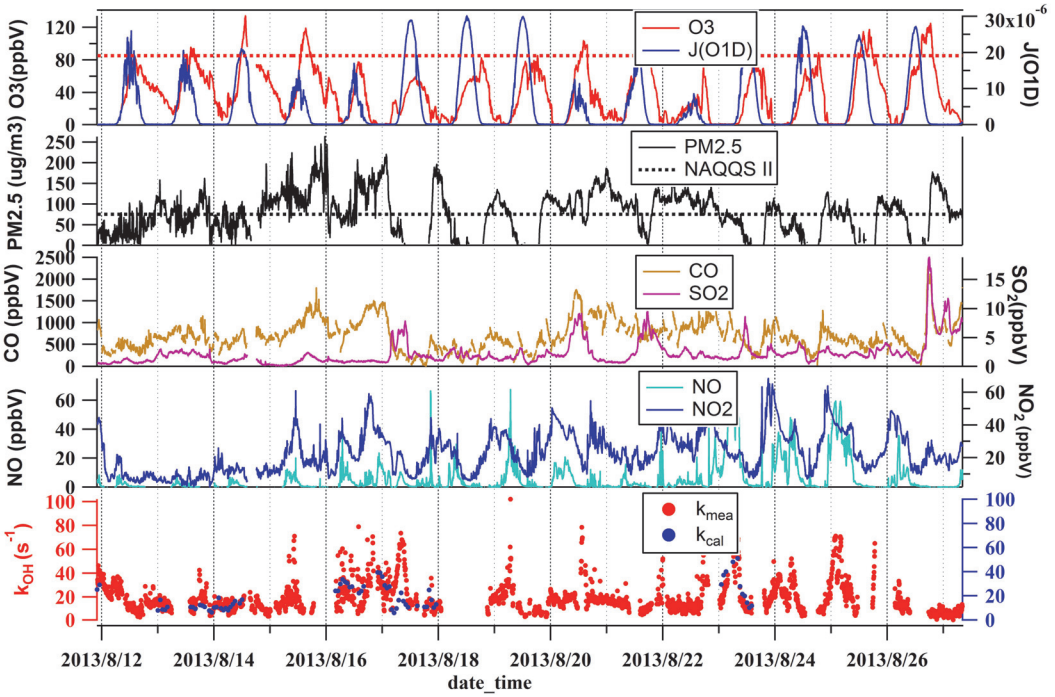


876 Fig 5-a Time series of meteorological parameters and inorganic trace gases during
877 August 2013 in Beijing.
878 Red and black dashed lines are Grade II of National Ambient Air Quality Standard.
879

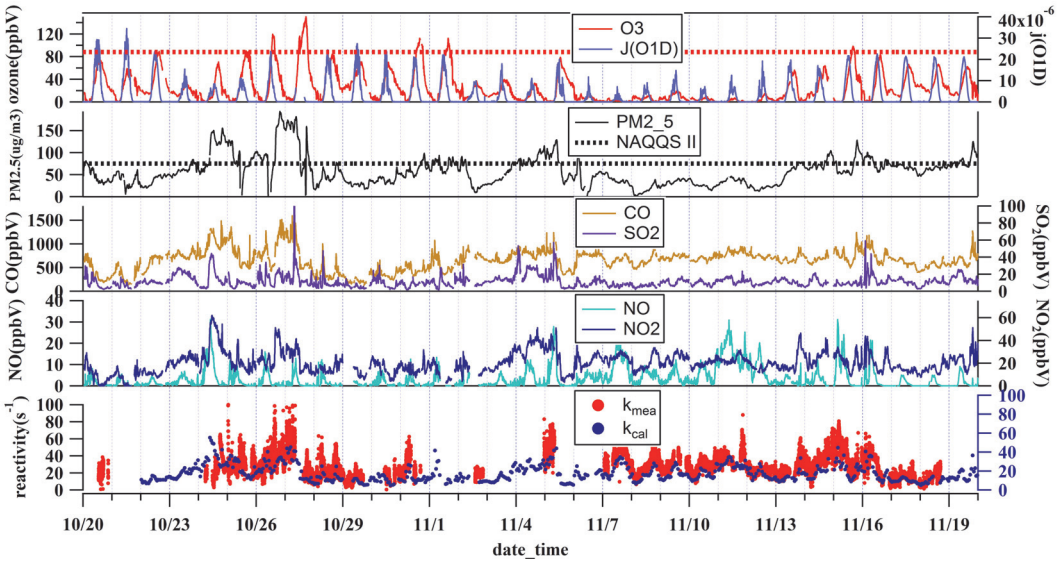


880 Fig 5-b Time series of meteorological parameters and inorganic trace gases during
881 October-November, 2014 in Heshan.
882 Red and black dashed lines are Grade II of National Ambient Air Quality Standard.
883
884

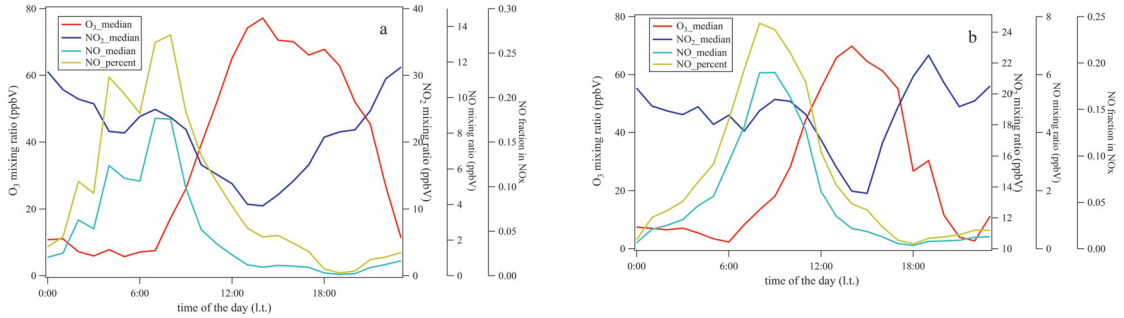


885 Fig 6 Diurnal variations of $O_3$, NO, $NO_2$ and relative contribution of NO to $NO_x$
886 in Beijing 2013 (a) and Heshan 2014 (b)
887

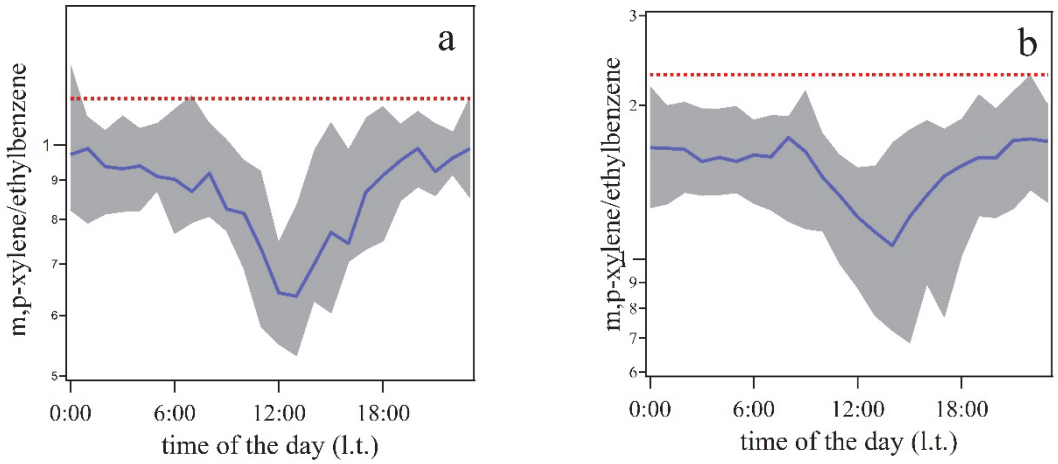


888

889 Fig 7 Ratios of m,p-xylene to ethylbenzene in Beijing 2013 (a) and Heshan 2014 (b)
890 Red dots line: the highest m,p-xylene to ethylbenzene ratio, assumed as emission
891 ratios of m,p-xylene to ethylbenzene, 1.15 ppbV $ppbV^{-1}$ in Beijing 2013 (a) and 2.3
892 ppbV $ppbV^{-1}$ in Heshan 2014 (b).
893 Shaded regions: Standard deviation for the ratios during the campaign average.
894

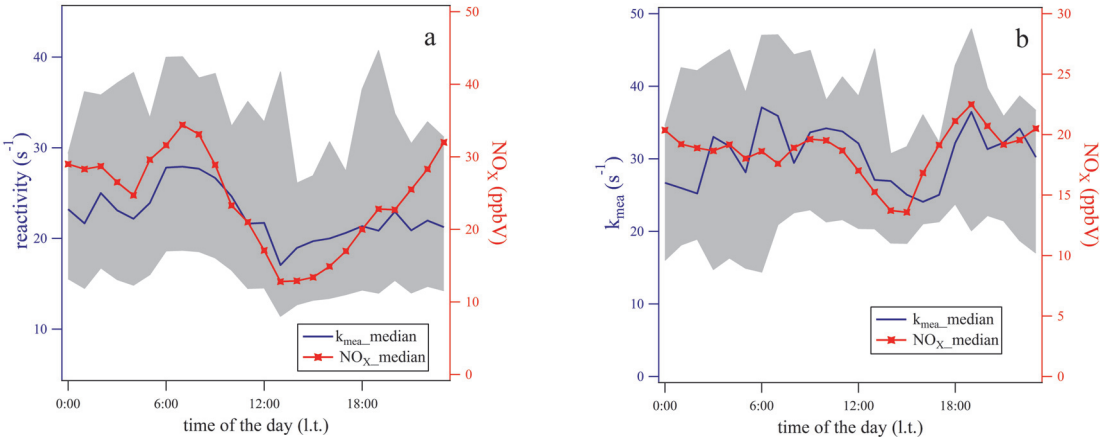


895

896 Fig 8 Diurnal variation of hourly median results of measured OH reactivity and $NO_x$
897 mixing ratios in Beijing (a) and Heshan (b)

898

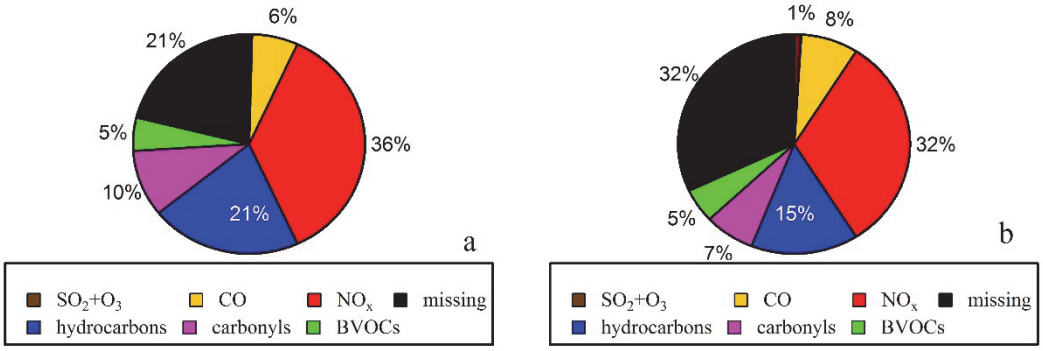


899 Fig 9 Composition of measured reactivity in Beijing (a) and Heshan (b)

900

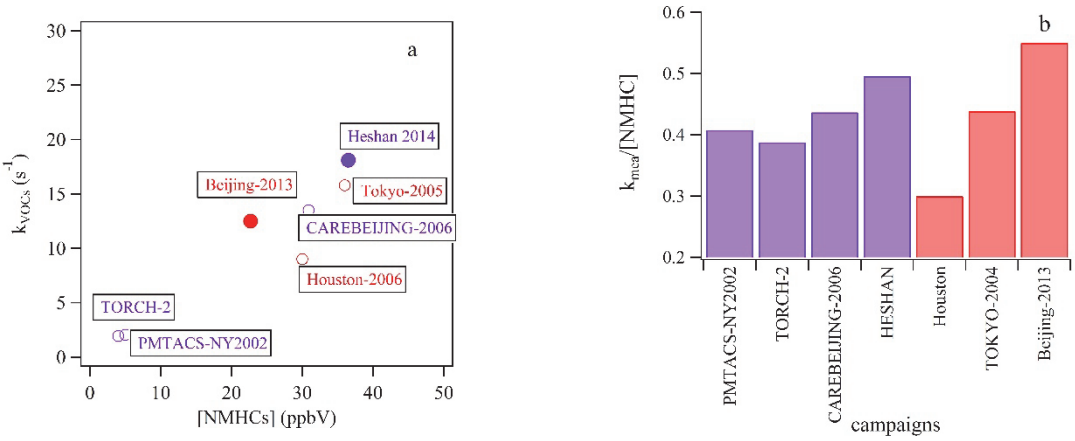


901

902 Fig 10 a: Comparison of VOCs reactivity and measured NMHCs in urban and
903 suburban observations.
904 b: Comparison of the ratio between VOCs reactivity and measured NMHCs in urban
905 and suburban observations

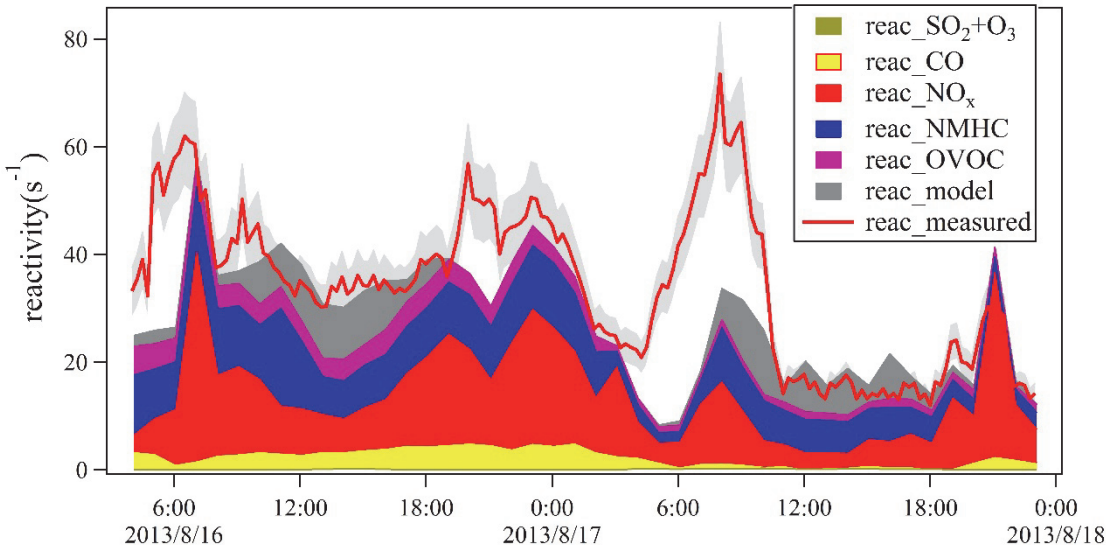


906

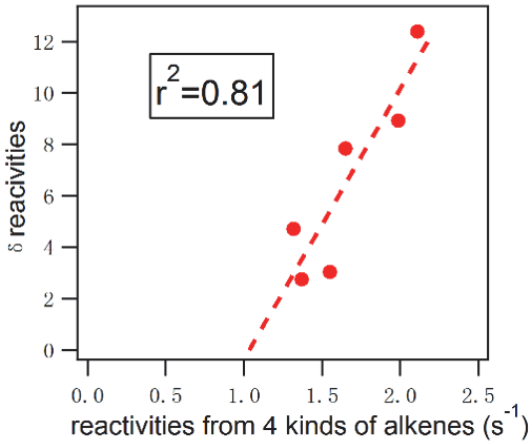


907

908 Fig 11 Upper panel: Comparison between measured and calculated reactivity in
909 Beijing August 16th to 18th 2013.
910 Shallow shaded region: uncertainty of measured reactivity. The same shallow shaded
911 region in Fig 12 represents the same.
912 Lower panel: Correlation between missing reactivity measured in 2013 and reactivity
913 assumed from branched-chain alkenes from 2005 in diurnal patterns. The 4
914 branched-alkenes are iso-butene, 2-methyl-1-butene, 3-methyl-1-butene and
915 2-methyl-2-butene.
916

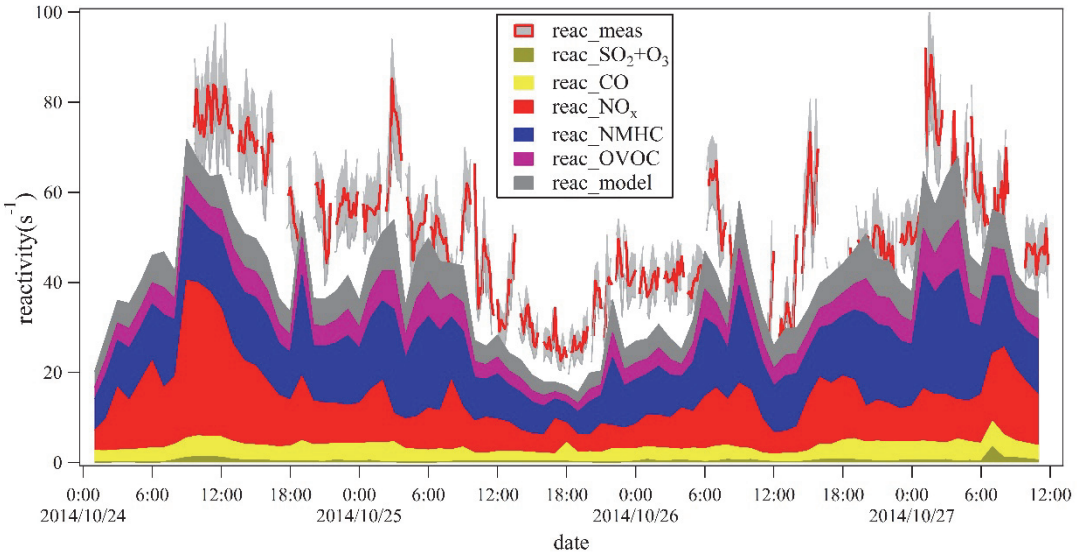


Fig 12 Comparison between measured reactivity and calculated reactivity as well as modelled reactivity in Heshan between October 24th and 27th 2014.

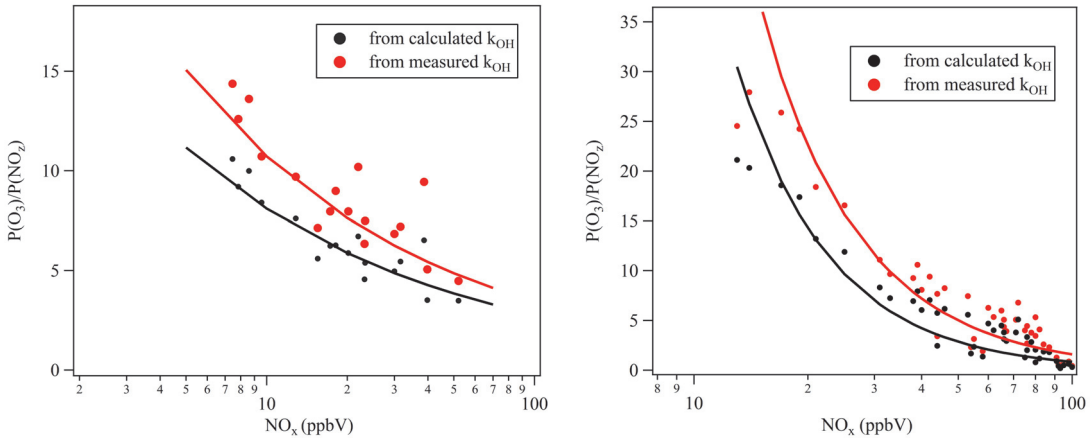


a b

Fig 13 Comparison between OPE calculated from measured reactivity and calculated reactivity in Beijing (a) and Heshan (b).

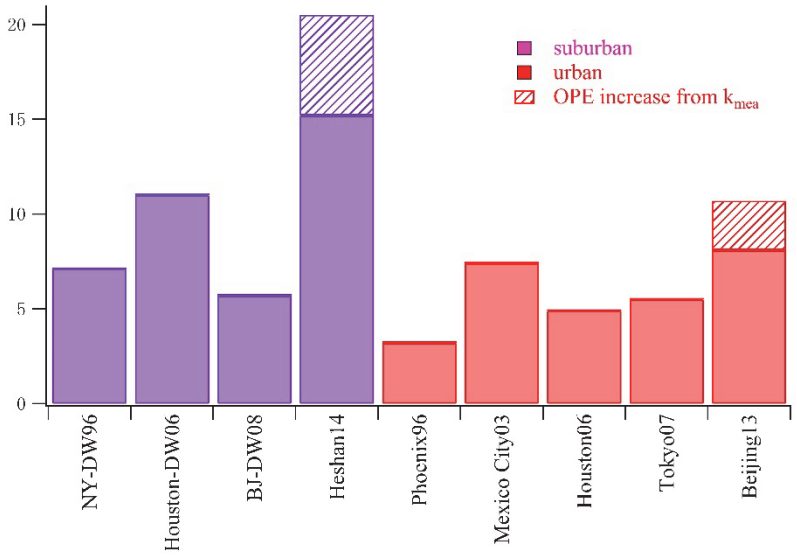


927

928 Fig 14 Comparison between the OPE results in this study and other results from
929 literatures. The comparison is made with the $NO_x$ = 20 ppbV. "DW" is in abbreviation
930 of downwind.

931